Corresponding address: Centre for Earth Evolution and Dynamics (CEED), Department of Geosciences, University of Oslo, PO Box 1028, N-0315 Oslo, Norway

# Supporting Information for "A new tectono-magmatic model for the Lofoten/Vesterålen Margin at the outer limit of the Iceland Plume influence"

Asbjørn Johan Breivik[a,], Jan Inge Faleide[a], Rolf Mjelde[b], Ernst R. Flueh[c], Yoshio Murai[d]

[a]*Centre for Earth Evolution and Dynamics (CEED), Department of Geosciences, University of Oslo, Norway*
[b]*Department of Earth Science, University of Bergen, Norway*
[c]*IFM-Geomar, Leibniz-Institute for Marine Sciences, Kiel, Germany*
[d]*Institute of Seismology and Volcanology, Hokkaido University, Sapporo, Japan*

## 1. Introduction

The supplementary material documents the complete wide-angle seismic data set, interpretation, ray tracing, and travel-time fit. A large map of the region is shown in Figure 1, while profile and instrument locations are shown in Figure 2. Large versions of the gravity and magnetic anomaly maps are in Figures 3-4. All seismic data and models are shown in Figures 5-20. Seismic phases constraining the crystalline crust are indicated for each data set: $P_x$ sedimentary refraction, $P_{g1}$ upper basement refraction, $P_{g2}$ middle basement refraction, $P_{g3}$ lower basement refraction, and $P_{g4}$ lower crustal body refraction, $P_n$ upper mantle refraction, $P_C P$ top lower crustal body reflection, $P_G P$ various intra-basement reflections, and $P_M P$ Moho reflection. The velocity model is repeated here in Figure 21.

*Email addresses:* a.j.breivik@geo.uio.no (Asbjørn Johan Breivik )

## References

Berndt, C., Planke, S., Alvestad, E., Tsikalas, F., Rasmussen, T., 2001. Seismic volcanostratigraphy of the Norwegian Margin: constraints on tectonomagmatic break-up processes. J. Geol. Soc. 158, 413–426.

Jakobsson, M., Mayer, L. A., Coakley, B., Dowdeswell, J. A., Forbes, S., Fridman, B., Hodnesdal, H., Noormets, R., Pedersen, R., Rebesco, M., Schenke, H.-W., Zarayskaya, Y., Accettella, A. D., Armstrong, A., Anderson, R. M., Bienhoff, P., Camerlenghi, A., Church, I., Edwards, M., Gardner, J. V., Hall, J. K., Hell, B., Hestvik, O. B., Kristoffersen, Y., Marcussen, C., Mohammad, R., Mosher, D., Nghiem, S. V., Pedrosa, M. T., Travaglini, P. G., Weatherall, P., 2012. International Bathymetric Chart of the Arctic Ocean (IBCAO) Version 3.0. Geophys. Res. Lett. 39 (L12609).

Olesen, O., Ebbing, J., Lundin, E., Mauring, E., Skilbrei, J. R., Torsvik, T. H., Hansen, E. K., Henningsen, T., Midbøe, P., Sand, M., 2007. An improved tectonic model for the Eocene opening of the Norwegian-Greenland Sea: Use of modern magnetic data. Mar. Petrol. Geol. 24, 53–66.

Olesen, O., Gellein, J., Gernigon, L., Kihle, O., Koziel, J., Lauritsen, T., Mogaard, J. O., Myklebust, R., Skilbrei, J. R., Usov, S., 2010. Magnetic anomaly map, Norway and adjacent areas, 1:3 million.

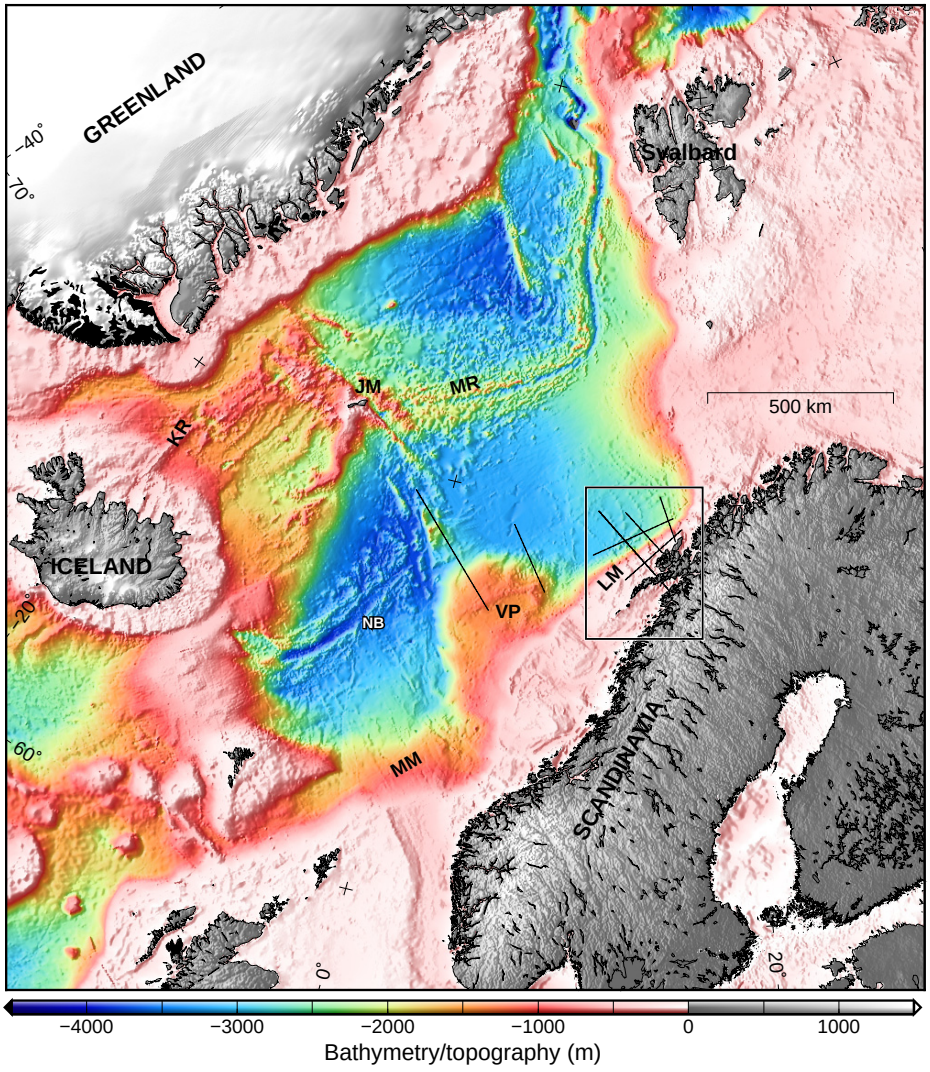


Figure 1: Bathymetry map with the location of the Euromargins 2003 OBS survey (lines inside box). VP: Vøring Plateau, JM: Jan Mayen, KR: Kolbeinsey Ridge, LM: Lofoten Margin, MM: Møre Margin, MR: Mohn Ridge, NB: Norway Basin.

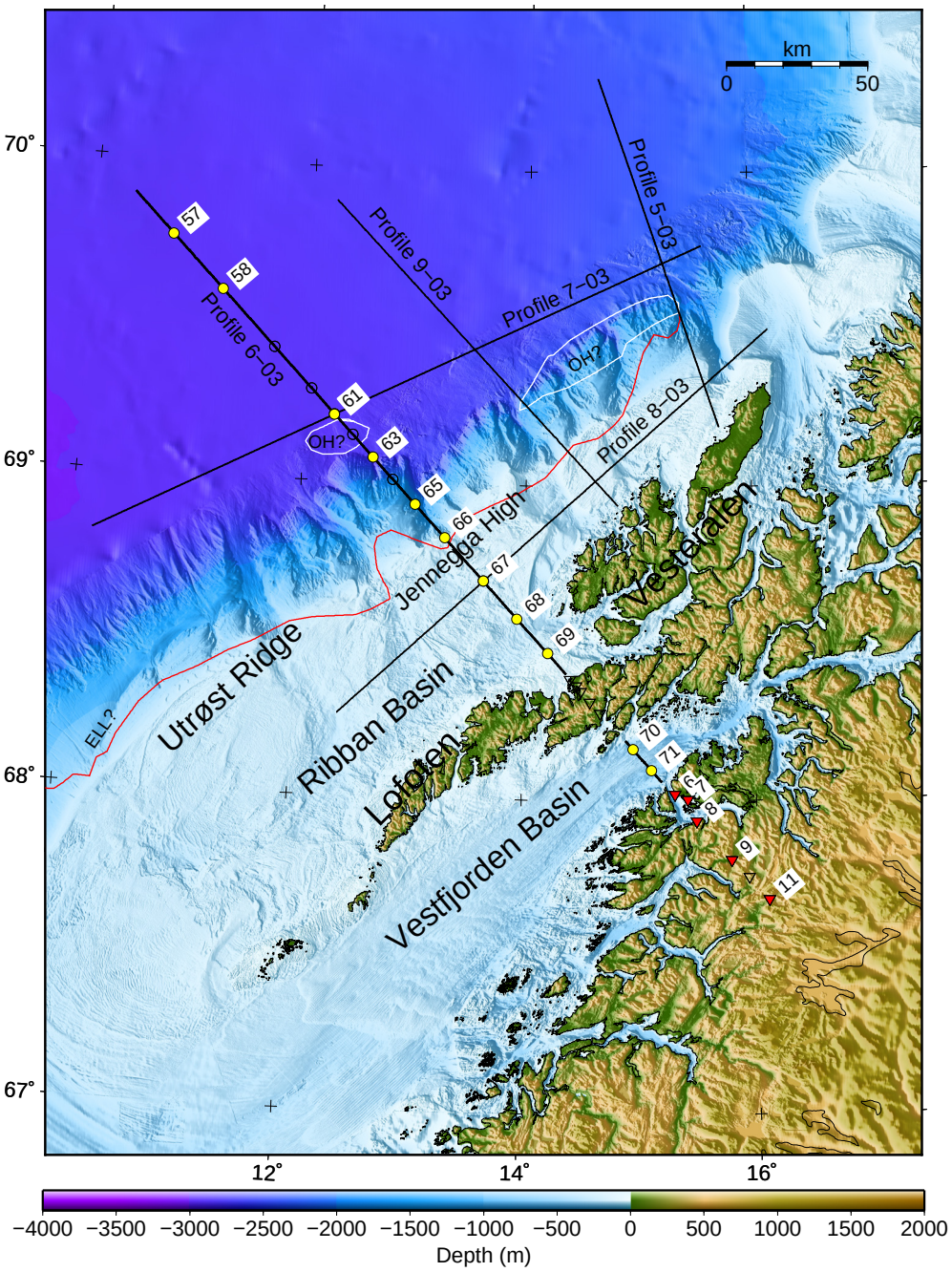


Figure 2: 200 m resolution topography and sidescan bathymetry based on 50 m resolution data from http://www.kartverket.no (©Kartverket) with Euromargins 2003 OBS lines. Deep ocean bathymetry is IBCAO v.3 (Jakobsson et al., 2012). OBS positions on Profile 6 (bold, black line) are shown with yellow-filled circles, and land stations with red-filled, inverted triangles. Unfilled symbols mark failed stations. Red line shows the proposed eastern limit of lava (ELL?), and white lines outer volcanic highs (OH?) from Berndt et al. (2001).

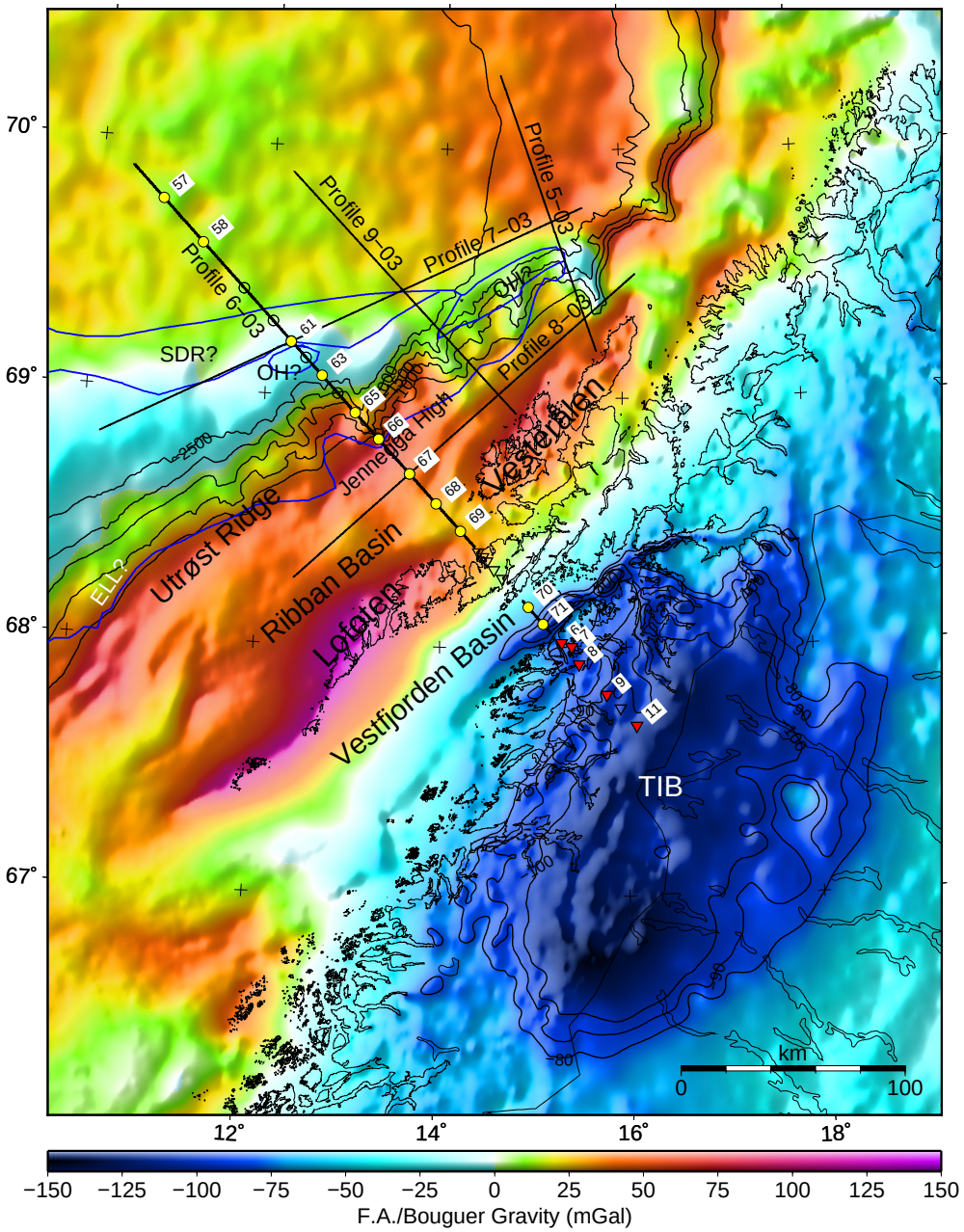


Figure 3: Free-air gravity (marine) and Bouguer gravity onshore with Euromargins 2003 OBS lines (Olesen et al., 2010). Swedish data ©Geological Survey of Sweden. Onshore contours show gravity values of -80, -90, and -100 mGal. Offshore contours show depth values at 500 m intervals. OBS positions on Profile 6 (bold, black line) are shown with yellow-filled circles, and land stations with red-filled, inverted triangles. White lines show magmatic interpretation from Berndt et al. (2001); ELL?: Eastern limit lava?, OH?: Outer volcanic highs?, SDR?: Seaward dipping reflector sequence?, TIB: Trans-Scandinavian Igneous Belt body.

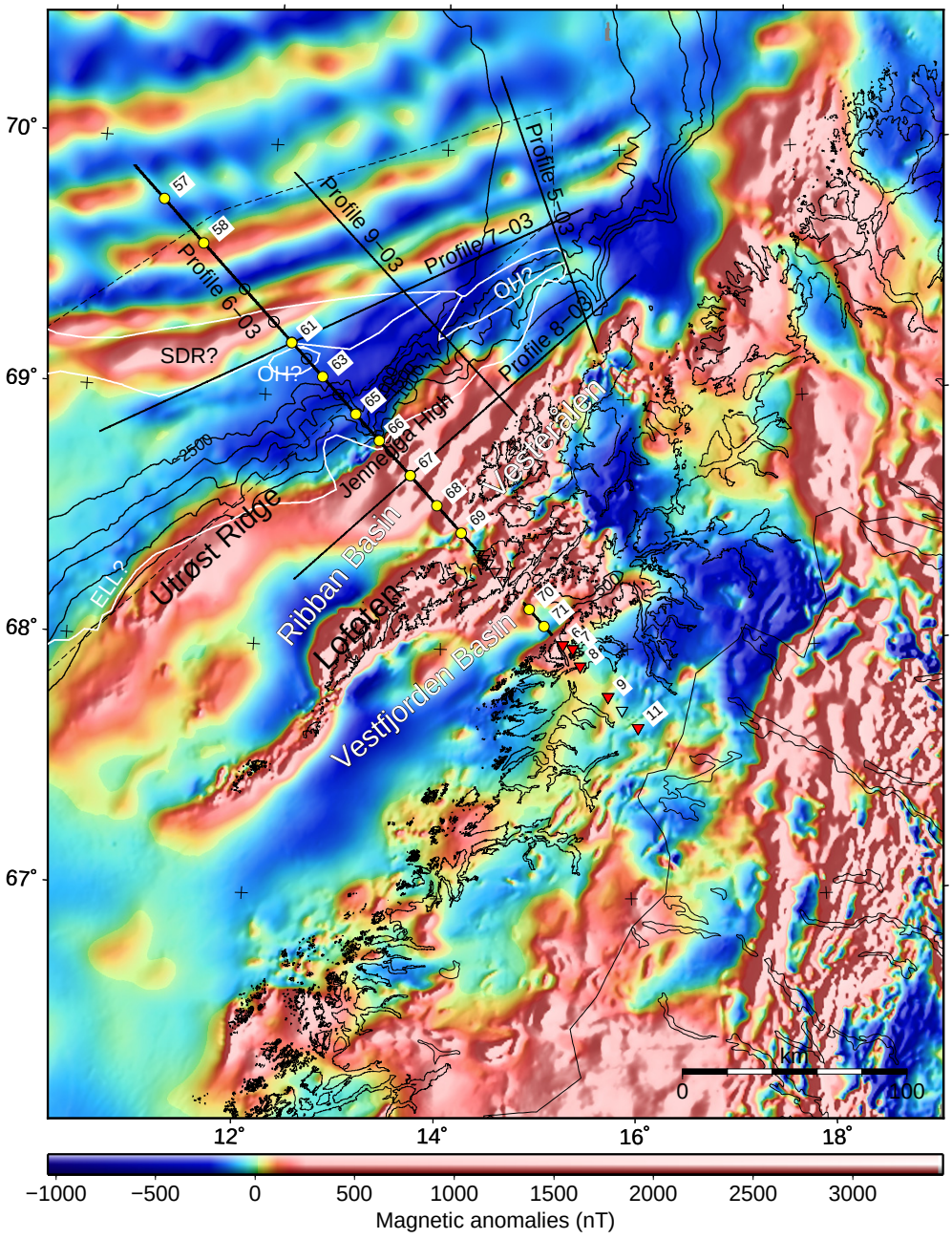


Figure 4: Regional magnetic anomalies (Olesen et al., 2007, 2010). Swedish data ©Geological Survey of Sweden. The new RAS-03 survey is indicated by the dashed line. Bathymetric contours at 500 m intervals are shown on top of both grids. Euromargins 2003 OBS lines are also shown, with OBS positions (yellow-filled circles) and land stations (red-filled, inverted triangles) on Profile 6-03. White lines show magmatic interpretation from Berndt et al. (2001); ELL?: Eastern limit lava?, OH?: Outer volcanic highs?, SDR?: Seaward dipping reflector sequence?, TIB: Trans-Scandinavian Igneous Belt body.

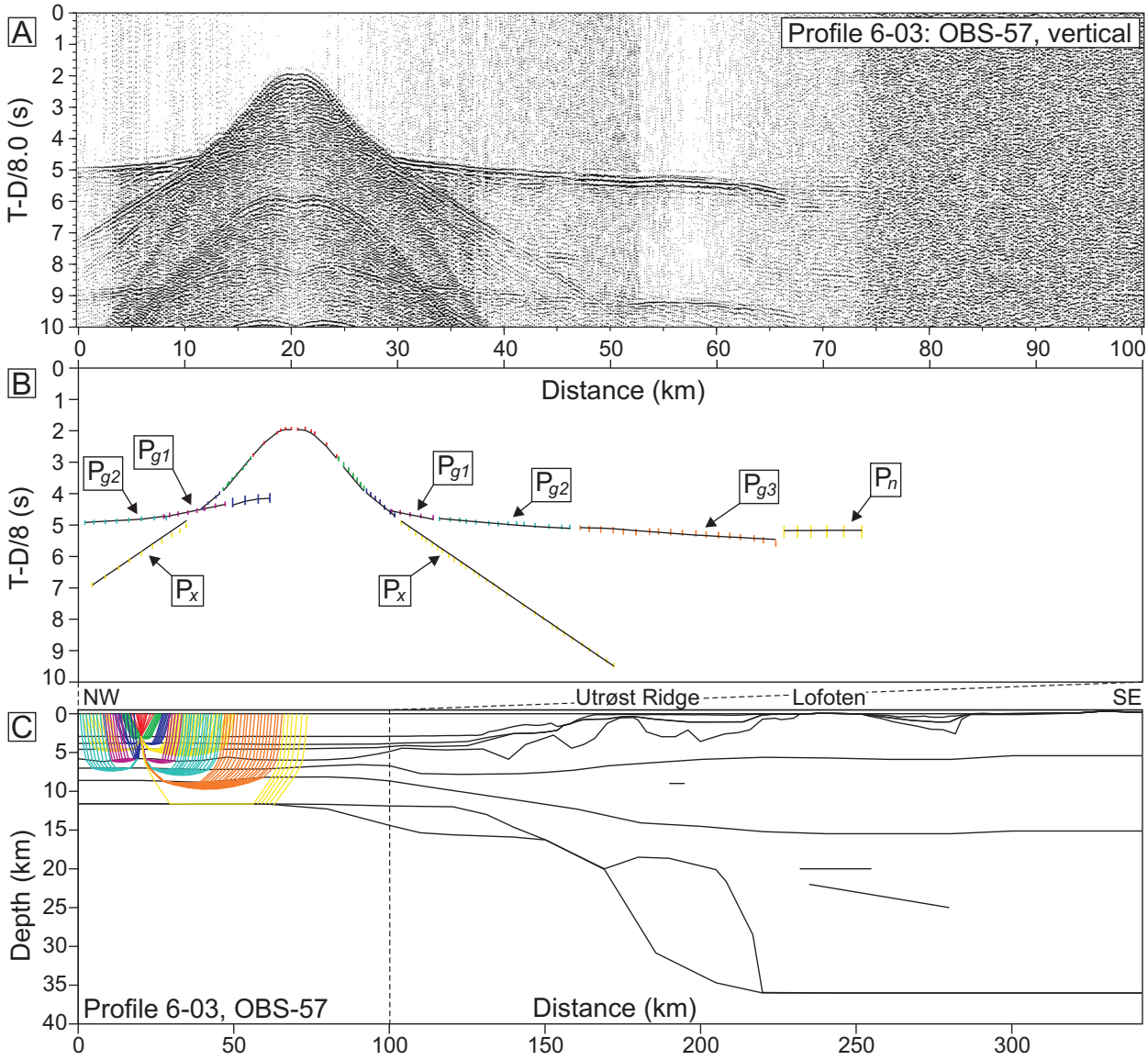


Figure 5: Data, interpretation, and ray tracing of OBS 57, Profile 6-03. A: OBS data, vertical component, offset-dependent scaling. B: Interpretation (vertical bars) and model prediction (solid lines). C: Ray tracing of the velocity model.

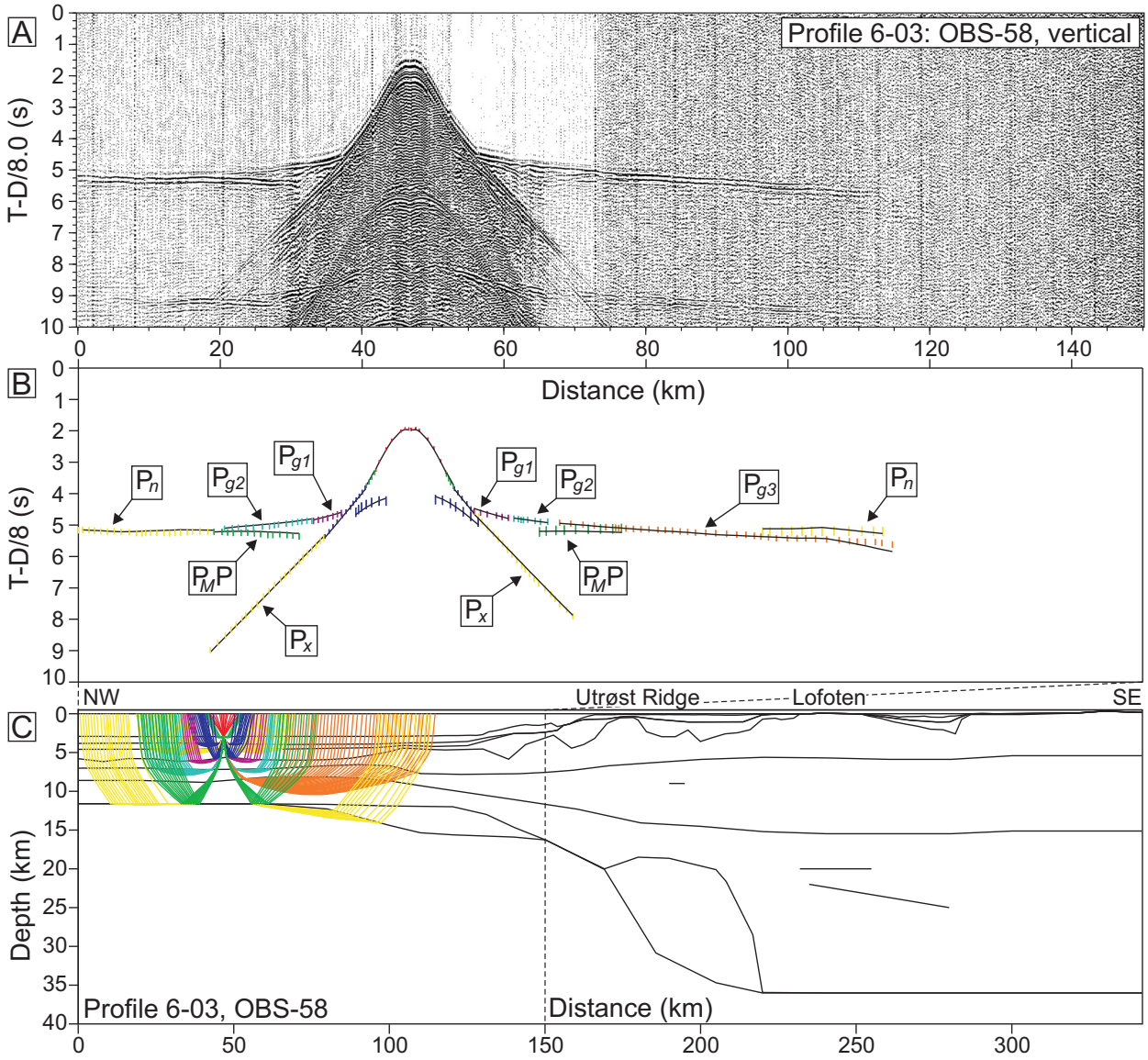


Figure 6: Data, interpretation, and ray tracing of OBS 58, Profile 6-03. A: OBS data, vertical component, offset-dependent scaling. B: Interpretation (vertical bars) and model prediction (solid lines). C: Ray tracing of the velocity model.

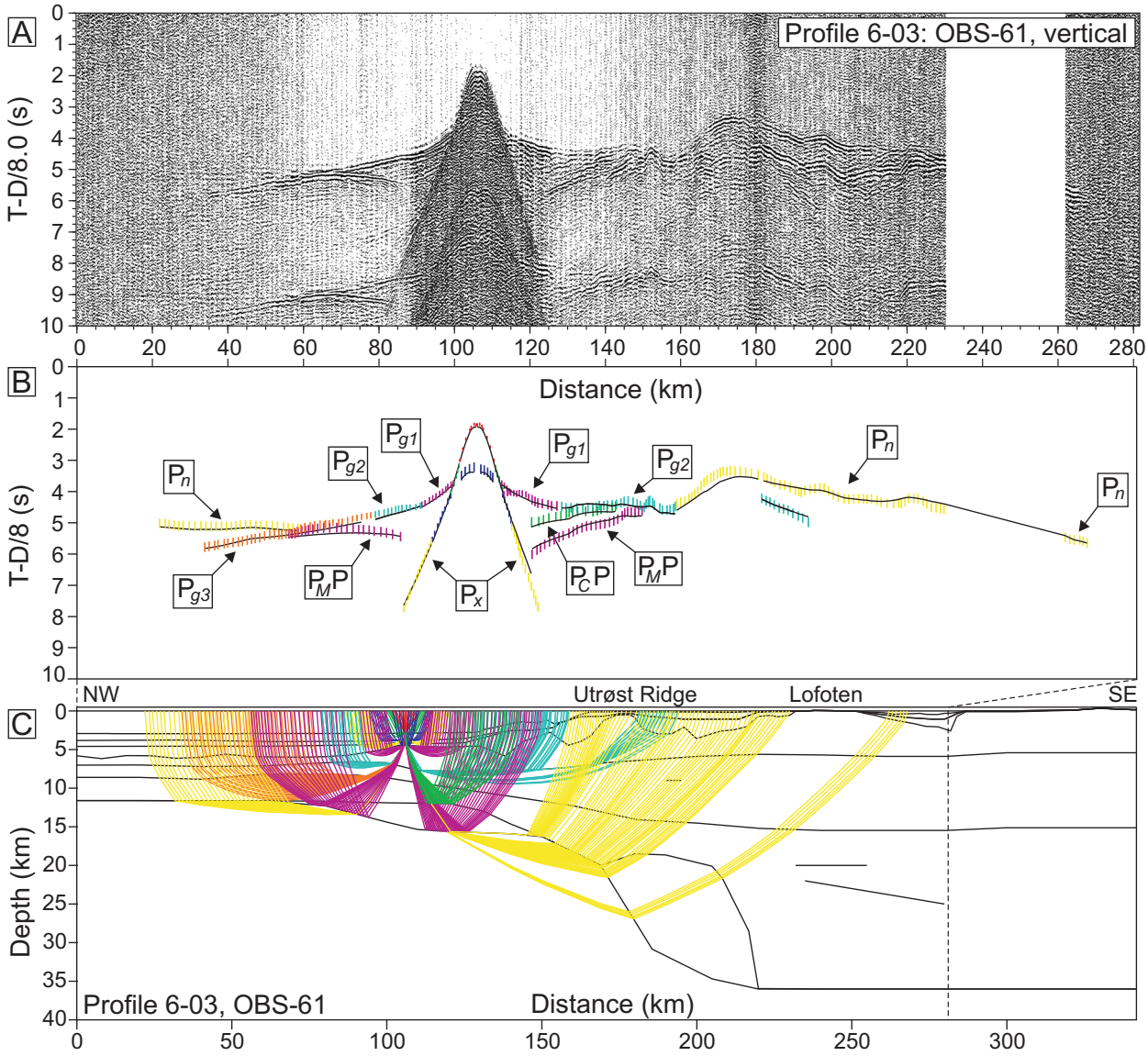


Figure 7: Data, interpretation, and ray tracing of OBS 61, Profile 6-03. A: OBS data, vertical component, offset-dependent scaling. B: Interpretation (vertical bars) and model prediction (solid lines). C: Ray tracing of the velocity model.

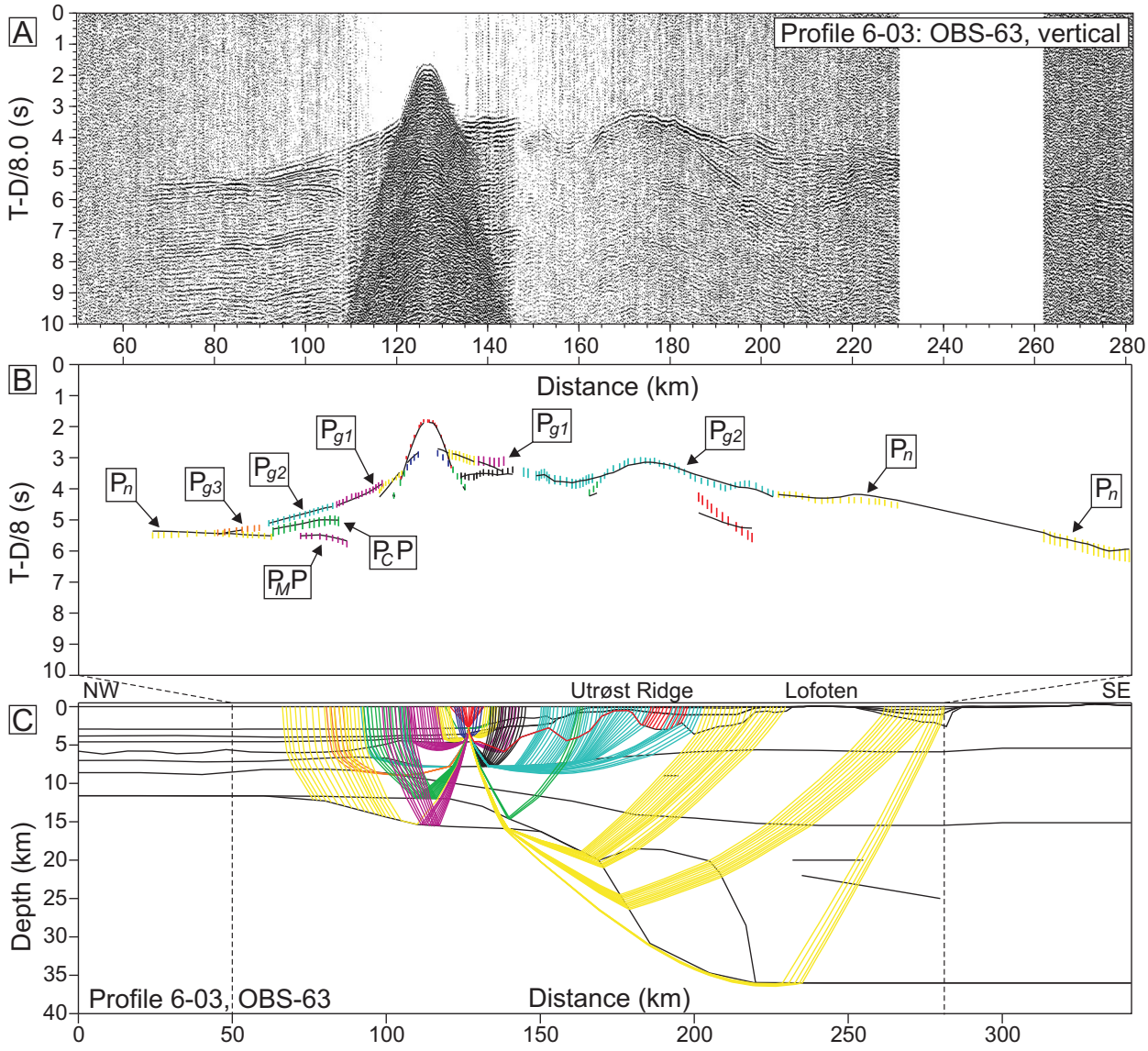


Figure 8: Data, interpretation, and ray tracing of OBS 63, Profile 6-03. A: OBS data, vertical component, offset-dependent scaling. B: Interpretation (vertical bars) and model prediction (solid lines). C: Ray tracing of the velocity model.

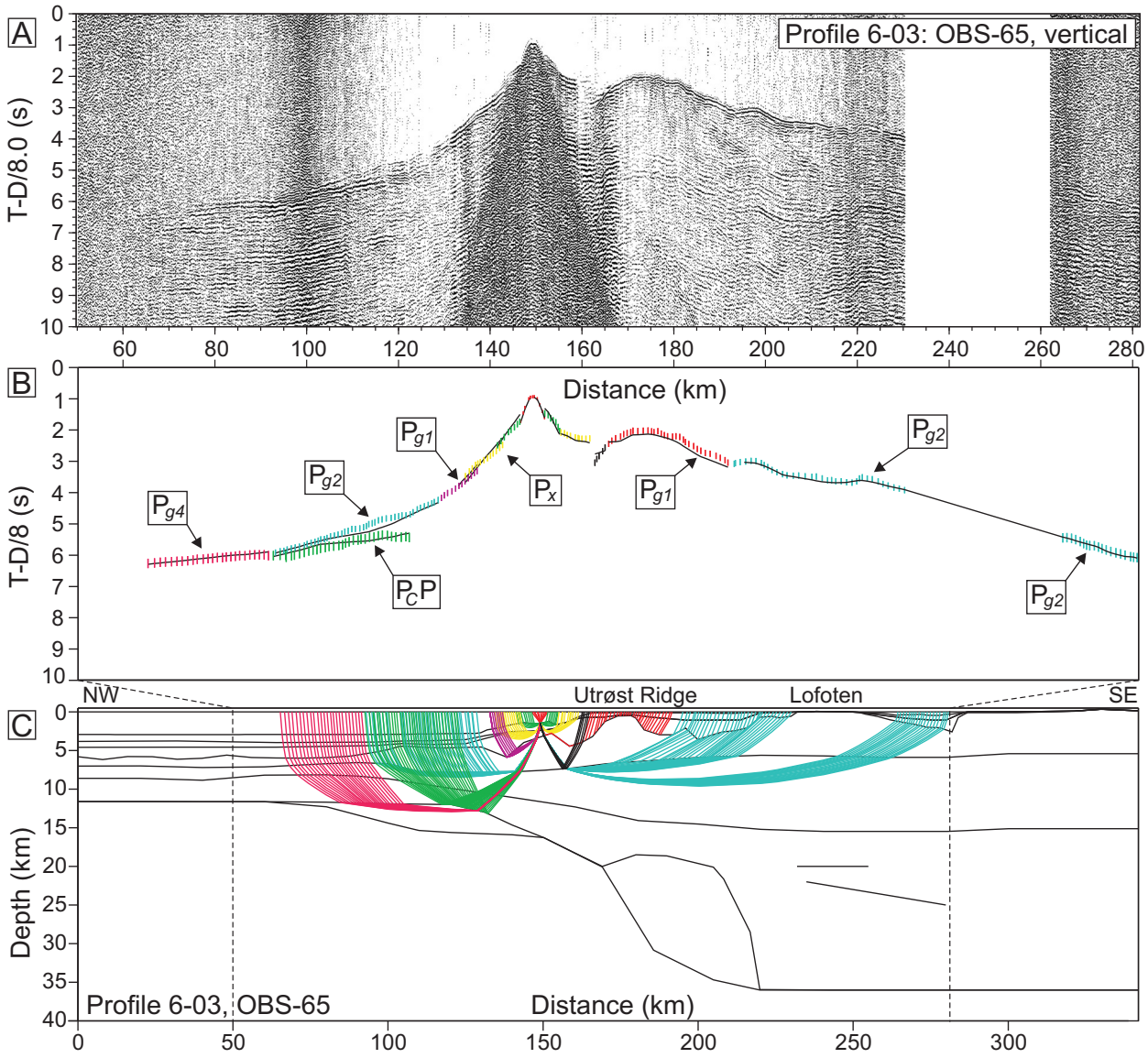


Figure 9: Data, interpretation, and ray tracing of OBS 65, Profile 6-03. A: OBS data, vertical component, offset-dependent scaling. B: Interpretation (vertical bars) and model prediction (solid lines). C: Ray tracing of the velocity model.

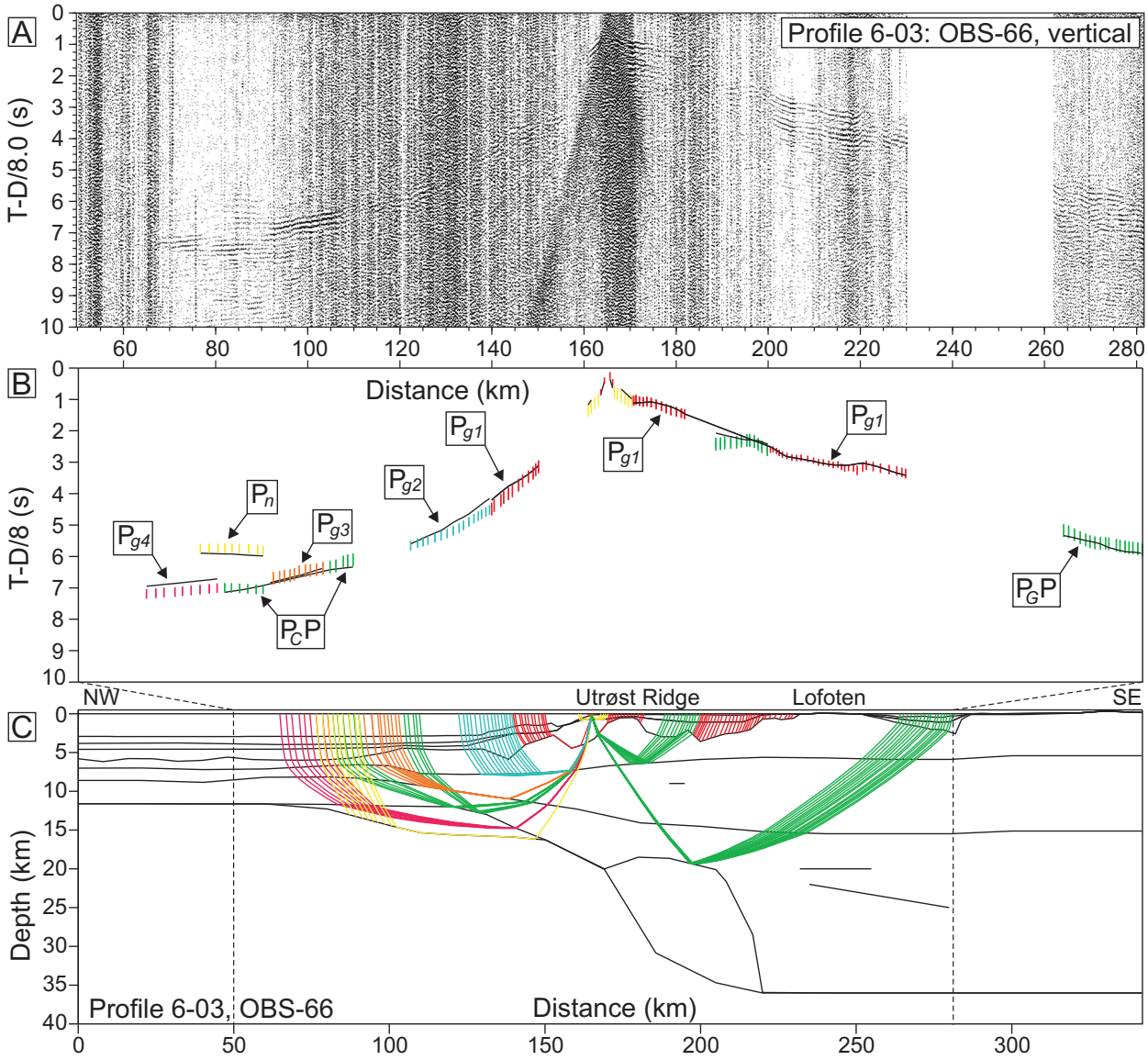


Figure 10: Data, interpretation, and ray tracing of OBS 66, Profile 6-03. A: OBS data, vertical component, offset-dependent scaling. B: Interpretation (vertical bars) and model prediction (solid lines). C: Ray tracing of the velocity model.

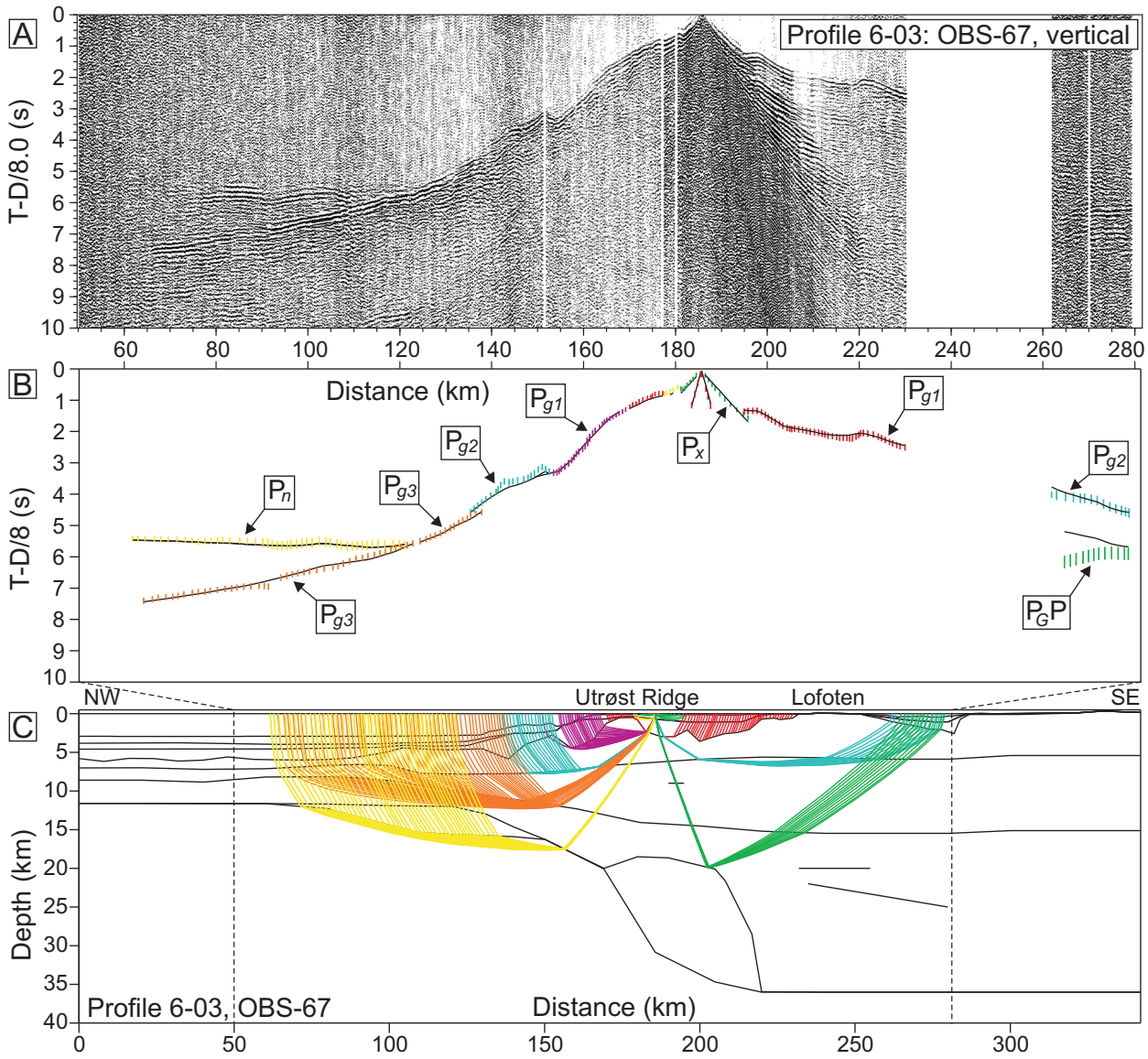


Figure 11: Data, interpretation, and ray tracing of OBS 67, Profile 6-03. A: OBS data, vertical component, offset-dependent scaling. B: Interpretation (vertical bars) and model prediction (solid lines). C: Ray tracing of the velocity model.

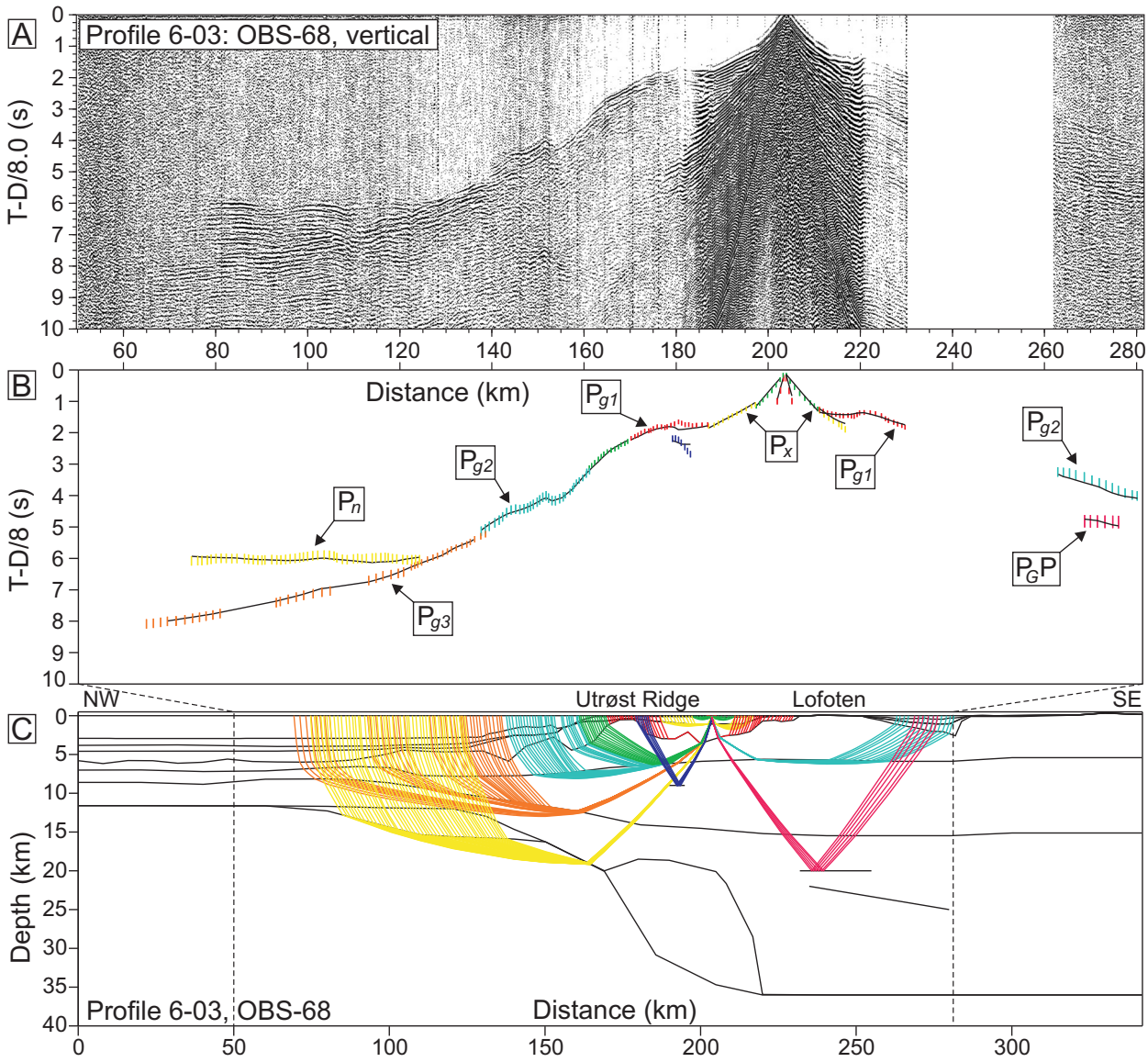


Figure 12: Data, interpretation, and ray tracing of OBS 68, Profile 6-03. A: OBS data, vertical component, offset-dependent scaling. B: Interpretation (vertical bars) and model prediction (solid lines). C: Ray tracing of the velocity model.

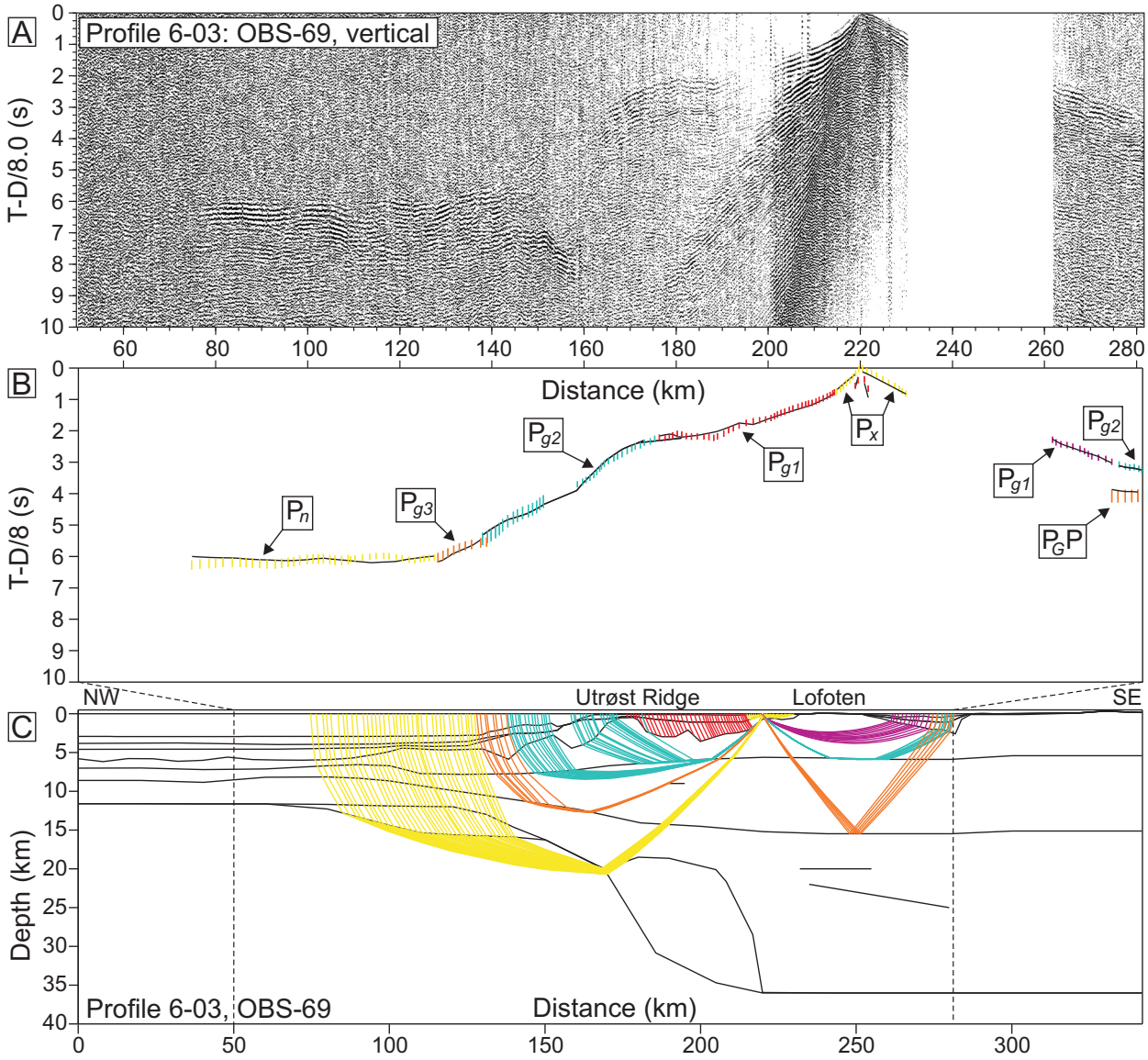


Figure 13: Data, interpretation, and ray tracing of OBS 69, Profile 6-03. A: OBS data, vertical component, offset-dependent scaling. B: Interpretation (vertical bars) and model prediction (solid lines). C: Ray tracing of the velocity model.

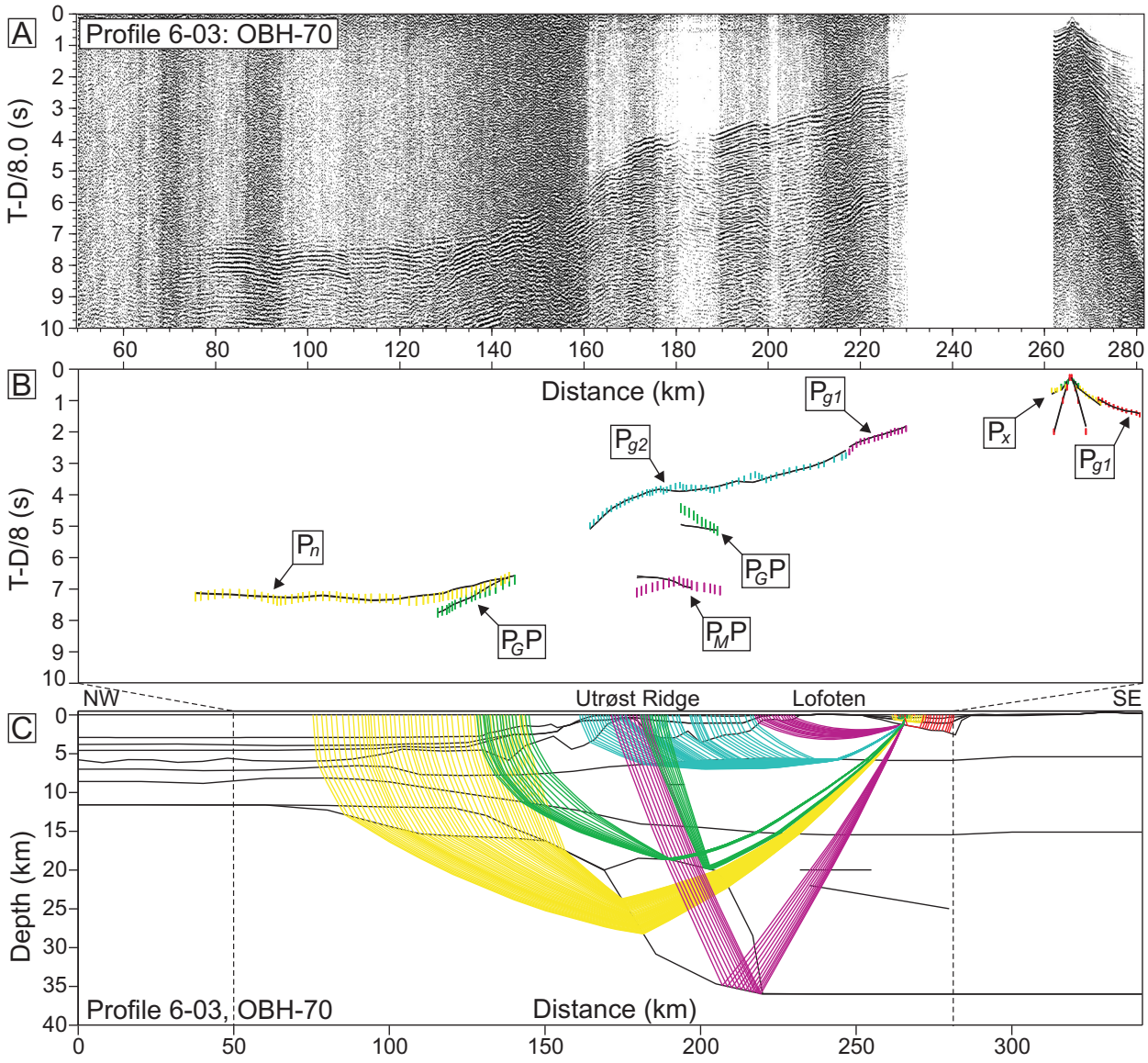


Figure 14: Data, interpretation, and ray tracing of OBH 70, Profile 6-03. A: Hydrophone data, offset-dependent scaling. B: Interpretation (vertical bars) and model prediction (solid lines). C: Ray tracing of the velocity model.

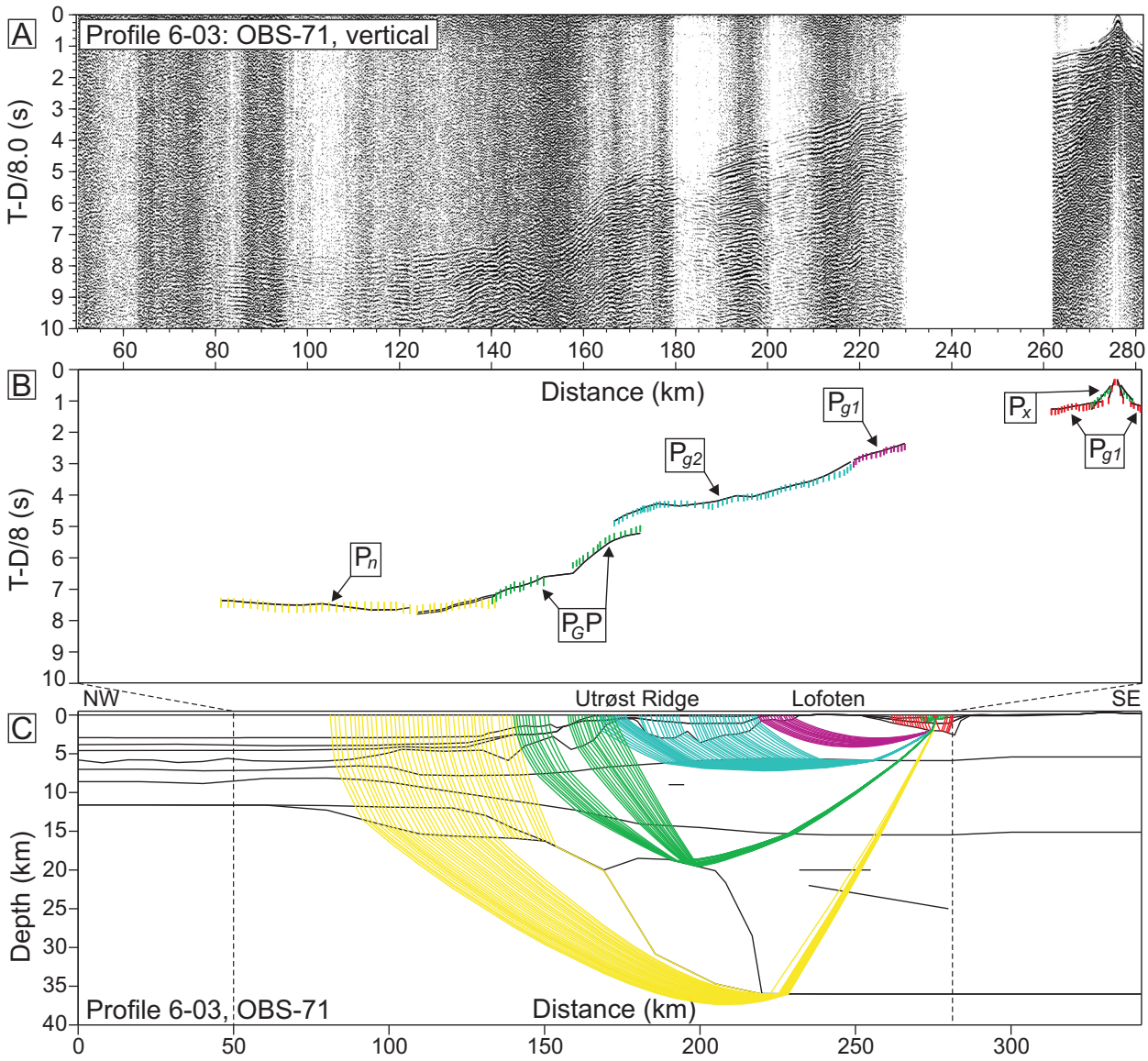


Figure 15: Data, interpretation, and ray tracing of OBS 71, Profile 6-03. A: OBS data, vertical component, offset-dependent scaling. B: Interpretation (vertical bars) and model prediction (solid lines). C: Ray tracing of the velocity model.

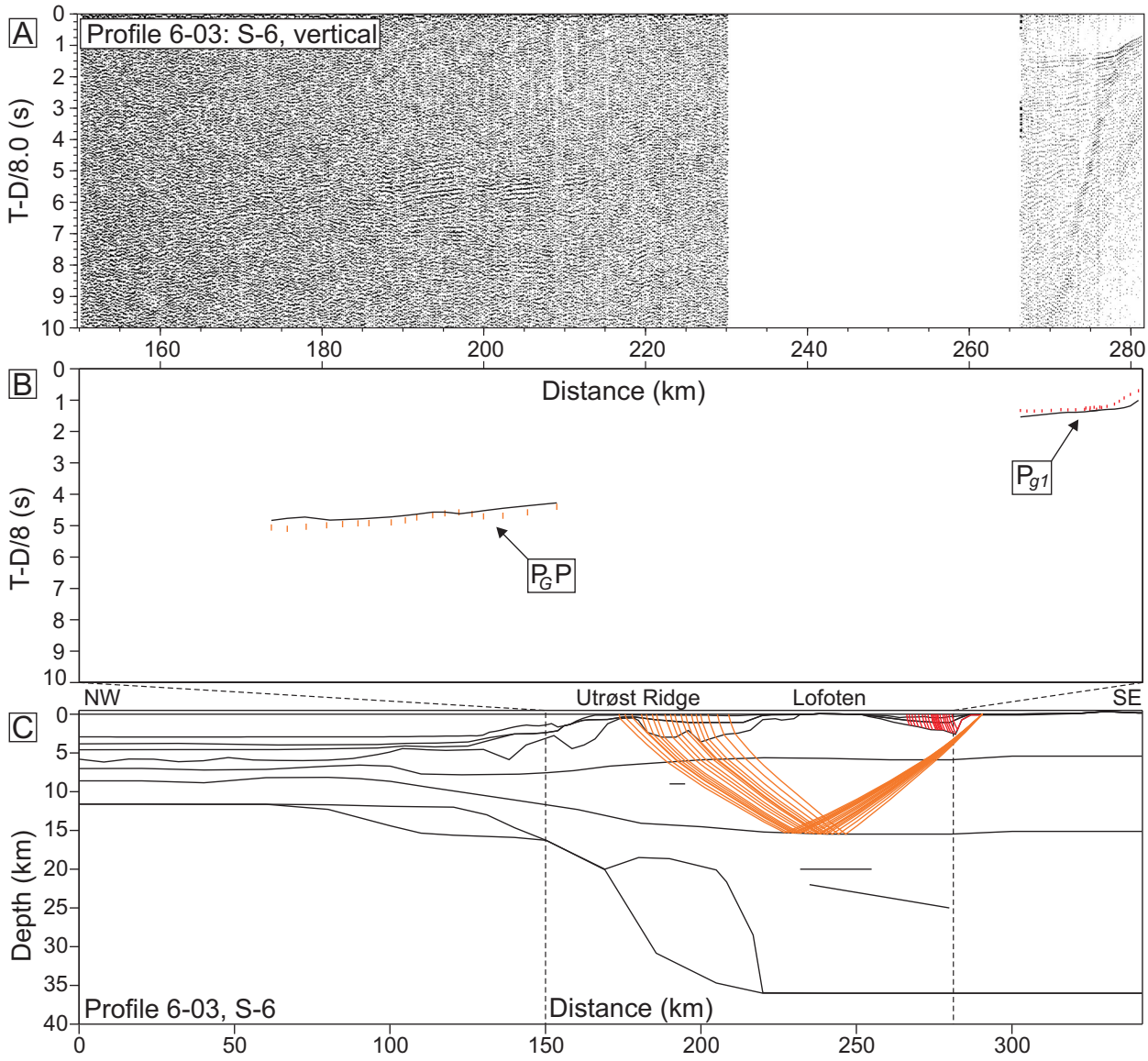


Figure 16: Data, interpretation, and ray tracing of land seismometer 6, Profile 6-03. A: Seismometer data, vertical component, offset-dependent scaling. B: Interpretation (vertical bars) and model prediction (solid lines). C: Ray tracing of the velocity model.

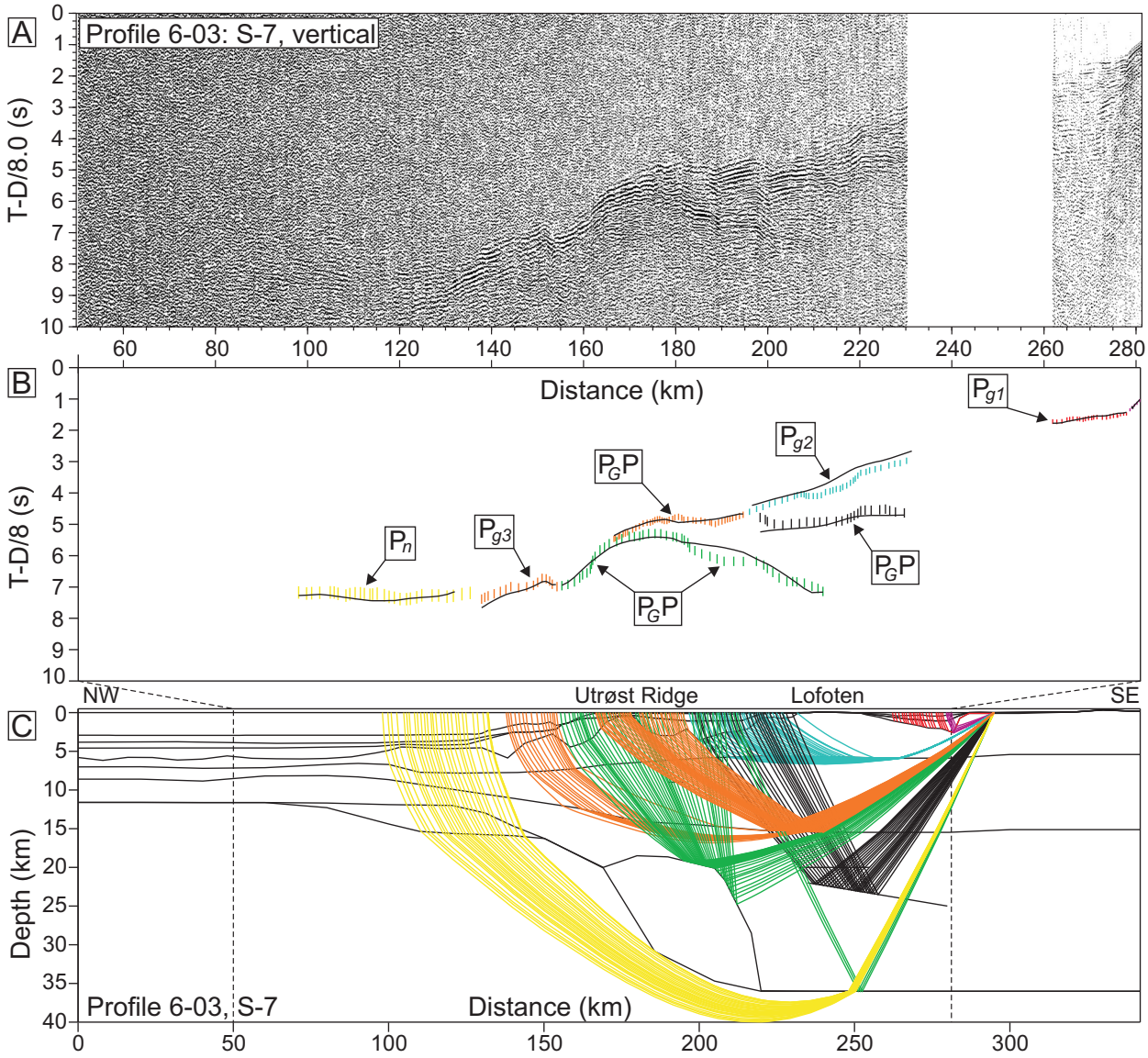


Figure 17: Data, interpretation, and ray tracing of land seismometer 7, Profile 6-03. A: Seismometer data, vertical component, offset-dependent scaling. B: Interpretation (vertical bars) and model prediction (solid lines). C: Ray tracing of the velocity model.

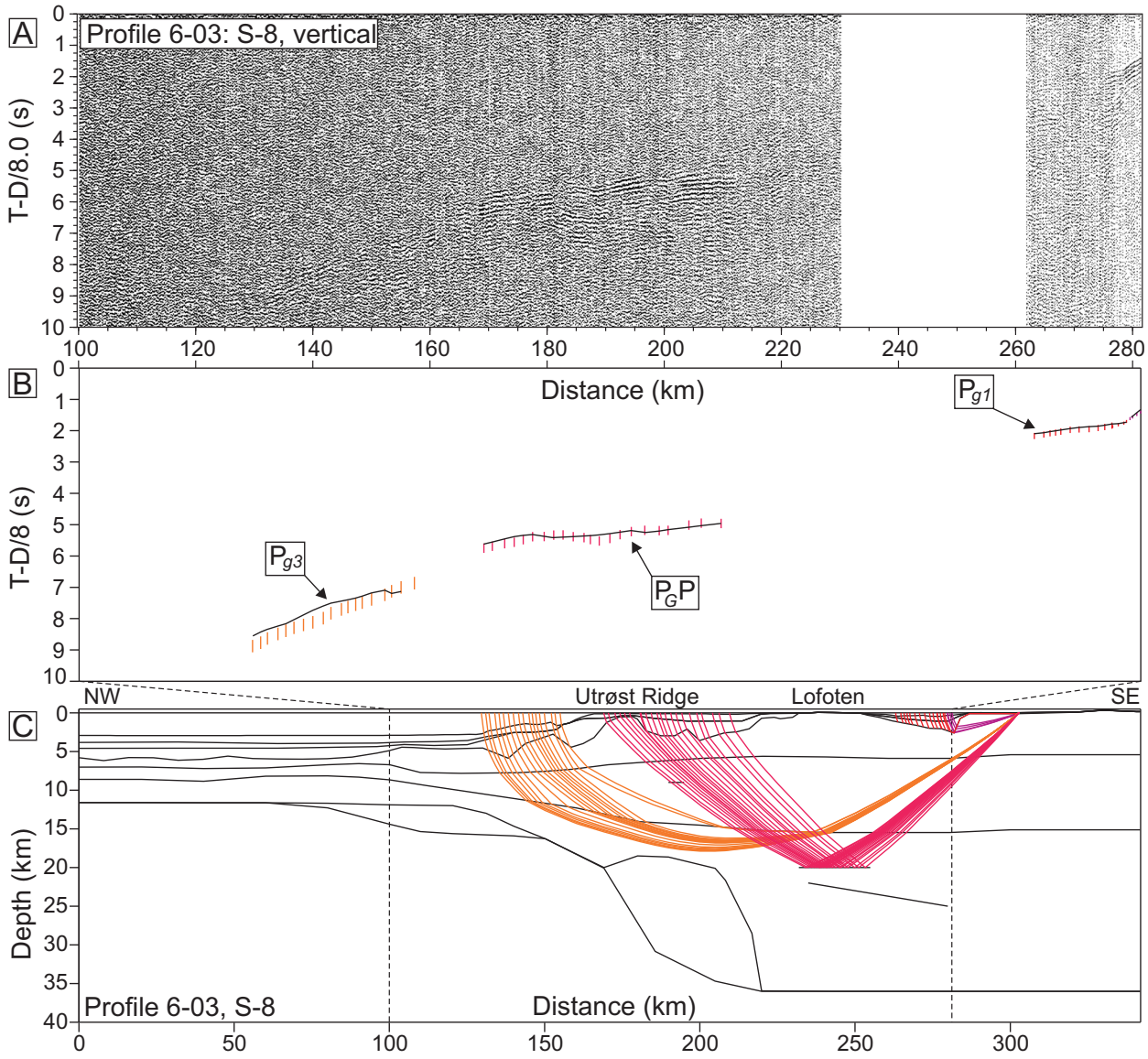


Figure 18: Data, interpretation, and ray tracing of land seismometer 8, Profile 6-03. A: Seismometer data, vertical component, offset-dependent scaling. B: Interpretation (vertical bars) and model prediction (solid lines). C: Ray tracing of the velocity model.

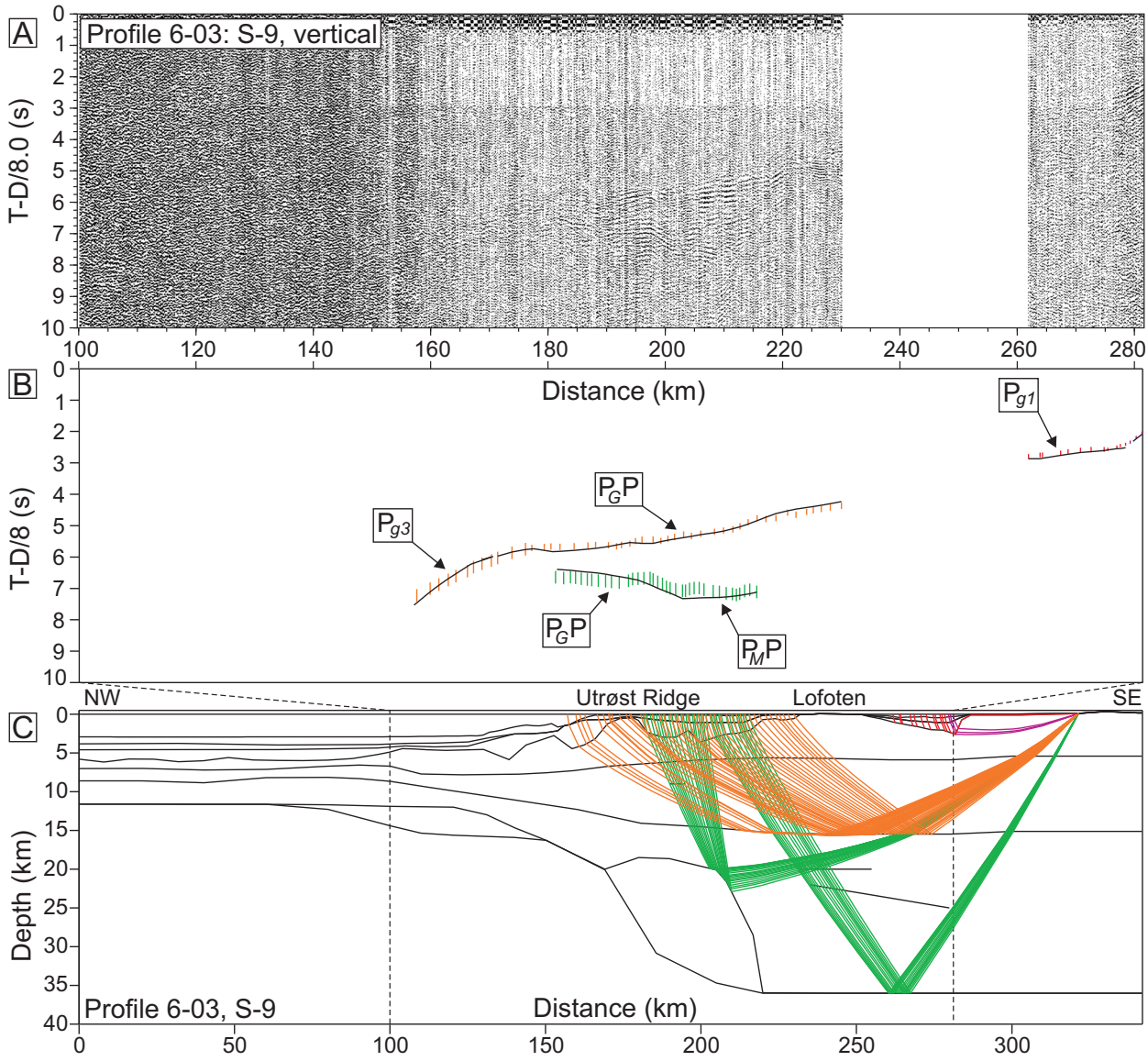


Figure 19: Data, interpretation, and ray tracing of land seismometer 9, Profile 6-03. A: Seismometer data, vertical component, offset-dependent scaling. B: Interpretation (vertical bars) and model prediction (solid lines). C: Ray tracing of the velocity model.

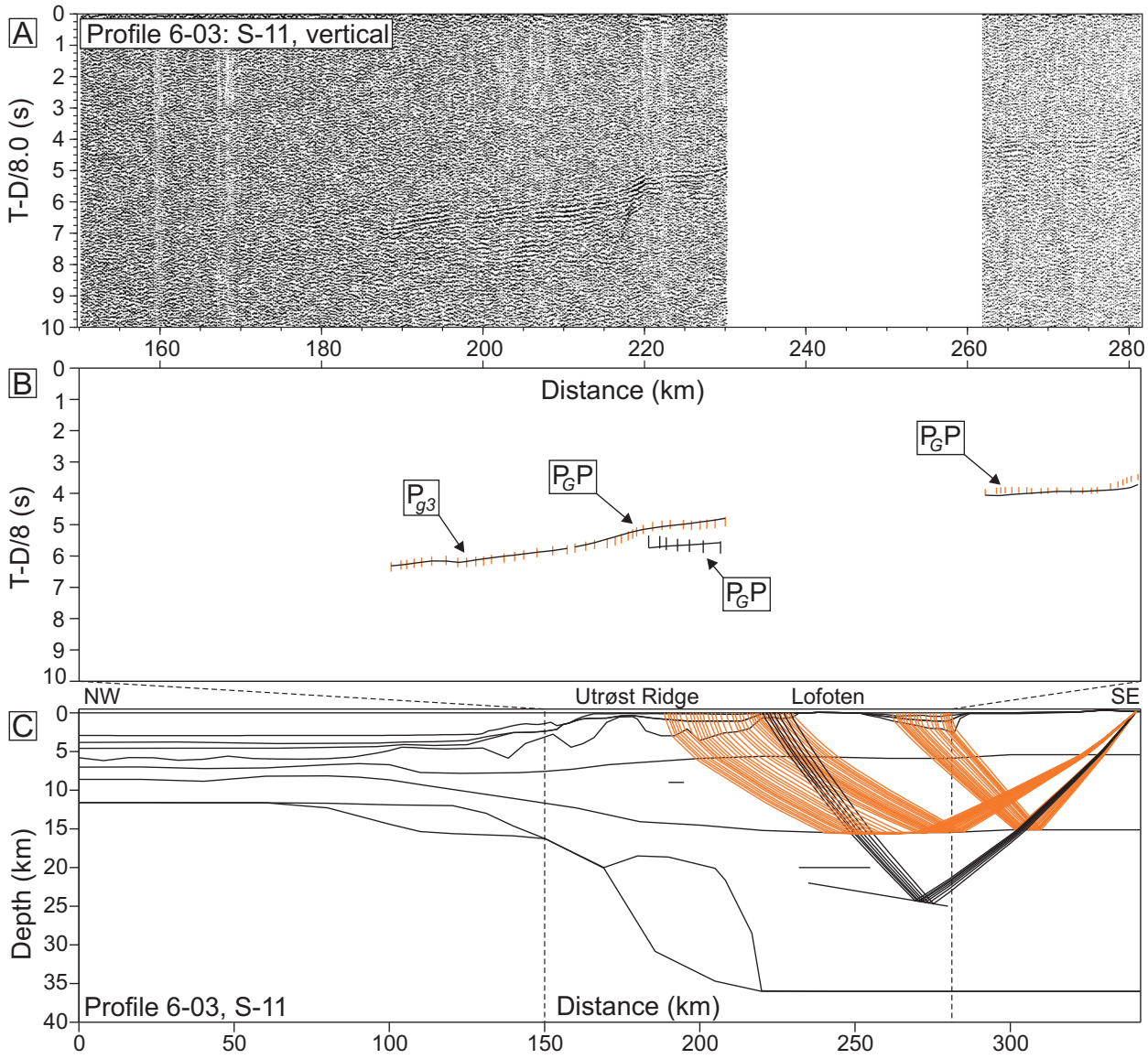


Figure 20: Data, interpretation, and ray tracing of land seismometer 11, Profile 6-03. A: Seismometer data, vertical component, offset-dependent scaling. B: Interpretation (vertical bars) and model prediction (solid lines). C: Ray tracing of the velocity model.

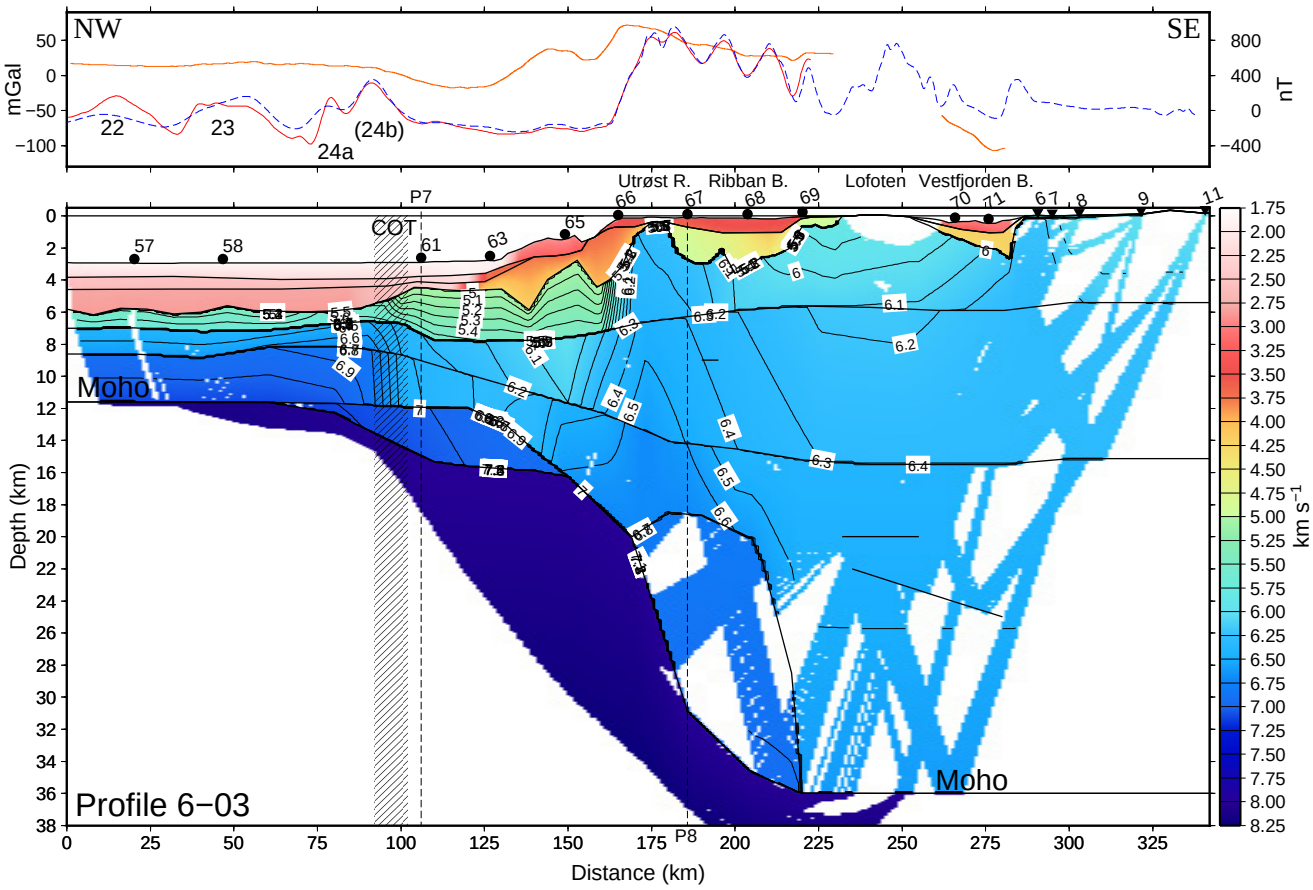


Figure 21: Gridded crustal velocity model of Profile 6-03, showing ray coverage. The OBS/H locations are numbered on the seafloor, and seismometers onshore. Hachures indicate the continent-ocean transition (COT). The magnetic (red solid line) and Free-air gravity (orange solid line) tracks collected along profile are shown above. The dashed blue line is extracted from the magnetic grid of Olesen et al. (2010).